Int. J. Radiation Oncology Biol. Phys., Vol. 62, No. 2, pp. 579–584, 2005

0360-3016/05/$–see front matter

ELSEVIER

doi:10.1016/j.ijrobp.2005.02.028

PHYSICS CONTRIBUTION

A DOSIMETRIC STUDY OF LEIPZIG APPLICATORS

José Pérez-Calatayud, Ph.D.,*† Domingo Granero, M.Sc.† Facundo Ballester, Ph.D.,† Vicente Puchades, M.Sc.‡ Emilio Casal, Ph.D.,†‖ Angela Soriano, M.Sc.,‖ and Vicente Crispín, M.Sc.§

*Radiotherapy Department, La Fe Hospital, Valencia, Spain; †Department of Atomic, Molecular, and Nuclear Physics, University of Valencia and IFIC-CSIC, Burjassot, Spain; ‡Grupo IMO-SFA, Madrid, Spain; ‖CND, Centro Nacional de Dosimetría, Valencia, Spain; §FIVO, Fundación Instituto Valenciano de Oncología, Valencia, Spain

Purpose: To obtain the absolute dose–rate distribution in liquid water for all six cup-shaped Leipzig applicators by means of an experimentally validated Monte Carlo (MC) code. These six applicators were used in high-dose-rate (HDR) afterloaders with the "classic" and v2 ^{192}Ir sources. The applicators have an inner diameter of 1, 2, and 3 cm, with the source traveling parallel or perpendicular to the contact surface.

Methods and Materials: The MC GEANT4 code was used to obtain the dose–rate distribution in liquid water for the six applicators and the two HDR source models. To normalize the applicator output factors, a MC simulation for the "classic" and v2 sources in air was performed to estimate the air-kerma strength. To validate this specific application and to guarantee that realistic source-applicator geometry was considered, an experimental verification procedure was implemented in this study, in accordance with the TG43U1 recommendations. Thermolumniscent dosimeter chips and a parallel plate ionization chamber in a polymethyl methacrylate (PMMA) phantom were used to verify the MC results for the six applicators in a microSelectronHDR afterloader with the "classic" source. Dose–rate distributions dependence on phantom size has been evaluated using two different phantom sizes.

Results: Percentage depth dose and off-axis profiles were obtained normalized at a depth of 3 mm along the central axis for both phantom sizes. A table of output factors, normalized to 1 U of source kerma strength at this depth, is presented. The dose measured in the PMMA phantom agrees within experimental uncertainties with the dose obtained by the MC GEANT4 code calculations. The phantom size influence on dose–rate distributions becomes significant at depths greater than 5 cm.

Conclusions: MC-detailed simulation was performed for the Nucletron Leipzig HDR applicators. The matrix data obtained, with a grid separation of 0.5 mm, can be used to build a dataset in a convenient format to model these distributions for routine use with a brachytherapy treatment planning system. **© 2005 Elsevier Inc.**

HDR, Dosimetry, Leipzig applicators, Monte Carlo, Brachytherapy.

INTRODUCTION

In recent years, there has been a significant increase in the use of high-dose-rate (HDR) afterloader machines because of the changeover from traditional ^{137}Cs/^{192}Ir low-dose-rate brachytherapy. In addition, the use of orthovoltage X-ray machines for treatment of small superficial targets has decreased to minimum levels, mainly because of a lack of technical support and advancements in other systems, although recently, some manufacturers have begun to produce machines that incorporate the latest technology. As a result, small superficial malignancies are usually treated with megavoltage electron beams on linacs. In most cases, they are difficult to treat because of the small size and shallow depth of the tumor, requiring bolus in a critical setup, in addition to specific dosimetric measurements because the percentage depth dose changes drastically with field sizes smaller than the practical range. An alternative treatment for these small surface lesions is the use of Leipzig applicators as accessories for the microSelectronHDR system (Nucletron, Veenendaal, The Netherlands) (1–3). These cup-shaped applicators limit the irradiation to the required area using tungsten shielding, allowing the treatment of skin tumors, the oral cavity, and vaginal cuff, for example. A set of six applicators is commercially available, with inner diameters of 1, 2, and 3 cm, in which the source has either a parallel or perpendicular orientation with respect to the treatment surface. The applicators are provided with a protective plastic cap, in

Reprint requests to Facundo Ballester, Ph.D., Department of Atomic, Molecular, and Nuclear Physics. University of Valencia, C/ Dr. Moliner 50, E-46100 Burjassot, Spain; Tel: (+34) 96354-4216; Fax: (+34) 96354-4581; E-mail: Facundo.Ballester@uv.es

Supported by Nucletron, which provided us with the details of sources and applicators. D.G. was funded by a V-Segles grant from the University of Valencia. This study was supported in part by the Generalitat Valenciana (projects No. GV04B-212 and No. GRUPOS04/19). The authors acknowledge Clinica Benidorm for its research support.

Received Oct 13, 2004, and in revised form Feb 15, 2005. Accepted for publication Feb 16, 2005.

contact with the surface of the skin, to reduce the surface dose from electron contamination in the walls (4). As pointed out by Evans *et al.* (4), lesions should be less than 25 mm in diameter, with a smooth surface, and located in a region where contact with the entire applicator surface is possible.

Because of the scatter in the applicator wall and the air cavity between source and skin, the dose–rate distributions are different from those assumed by a treatment planning system for dosimetry calculations, where calculations are made with a free HDR source in an unbounded water phantom. Evans *et al.* (4) have measured the surface dose rate and percentage depth doses using a parallel-plate chamber in a polystyrene phantom and off-axis ratios with a diode in water and with film in a phantom. Hwang *et al.* (2) have measured output dose rates using a parallel-plate chamber at a depth of 3 mm in a polystyrene phantom and the percentage depth dose and off-axis distribution with a p-type diode in a water phantom.

The Monte Carlo (MC) method has been used frequently for brachytherapy dosimetric studies because of the advantages it presents with respect to experimental dosimetry as stated by TG43U1 (5). These include independence from detector positioning and response artifacts, smaller estimated uncertainty, and estimation of dose rate at longer and shorter distances. Its accuracy is mainly limited by geometric and elementary particle cross-section uncertainties, so the TG43U1 recommends a confirmation of MC results by experimental studies.

The purpose of this study is to obtain the absolute dose rate distributions in liquid water for the whole set of applicators using both source models in the microSelectronHDR afterloaders. This is done by means of an experimentally validated MC method. The data obtained are used to generate a dataset in a convenient format to allow the modeling of these distributions in a treatment planning system.

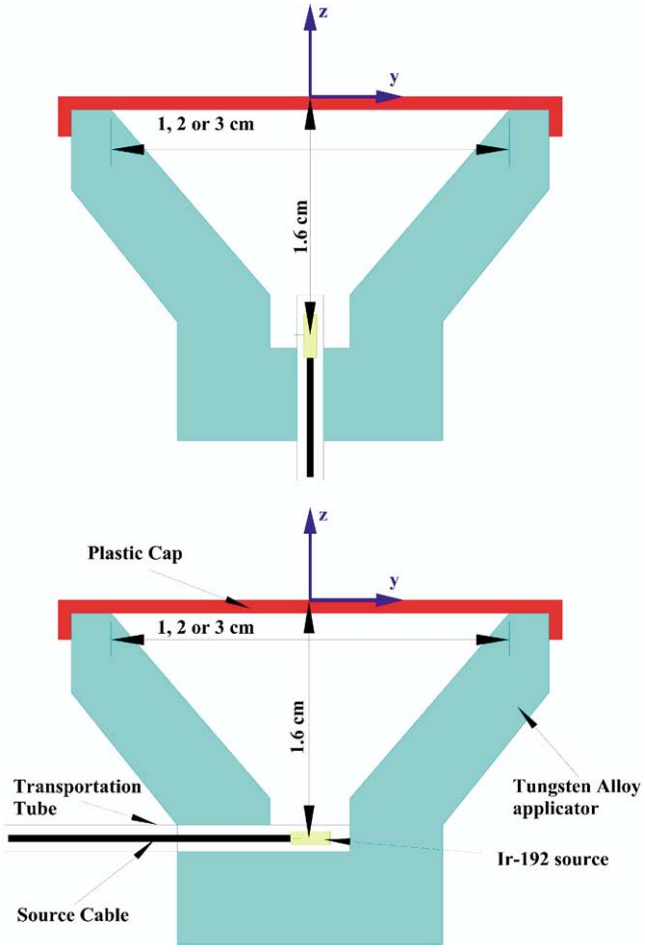

Fig. 1. Schematic view of a Leipzig horizontal-type applicator (bottom) and a vertical-type applicator (top). In vertical-type applicators, the source transportation tube is perpendicular to the treatment surface; the horizontal-type applicator is parallel to the treatment surface, but the source center for both orientations is the same. The coordinates system used is also shown.

METHODS AND MATERIALS

Leipzig applicators and HDR sources

There are six applicators with inner diameters of 1, 2, and 3 cm. Three of them use a source moving parallel to the treatment surface (H1, H2, and H3), whereas the remaining three use a source that moves perpendicularly to the treatment surface (V1, V2, and V3). They are each provided with a protective plastic cap 1-mm thick that is in contact with the surface of the skin.

There are two available source models that can be used with the microSelectronHDR in which the Leipzig applicators are incorporated: the "classic" source and the new v2 source, with an external diameter of 1.1 and 0.9 mm, respectively. The geometry and materials of the applicators and the sources have been fully included in the MC simulation using the technical data provided by the manufacturer (Fig. 1) and a photograph of the horizontal and vertical 3-cm diameter Leipzig applicators (H3 and V3) is shown in Fig. 2.

MC study of sources and applicators

The MC method was used to obtain the air-kerma strength and the dose rate in water around the sources being studied. The 4.6.0 version of the MC GEANT4 (6) code was used in this study. This code and the complete process involved in analyzing the data have been described in more detail in previous articles (7–9). Compton scattering and the photoelectric effect from the standard electromagnetic package, as well as Rayleigh scattering from the low-energy package of GEANT4, were used. The cutoff energy was 10 keV for photons.

The reference system used in this study is shown in Fig. 1, with the origin at the intersection of the applicator axis and the contact surface. The x and y axis are parallel to the surface and the positive z axis is directed toward the phantom. In all simulations, kerma was scored instead of dose because, at the ^{192}Ir energy, kerma approximates dose for distances greater than 1 mm from the source (10, 11). The linear track-length kerma estimator (12) was used to obtain kerma.

Air-kerma strength for the ^{192}Ir sources. To estimate the air-kerma strength for the "classic" and v2 sources, they were located in a $4 \times 4 \times 4$ m^3 dry air volume using cylindrical ring cells, 1-cm thick and 1-cm high, located along the transverse source axis. The air-kerma was scored from $r = 5$ cm to $r = 150$ cm, where r is the distance to the source along the transverse axis, using the linear track-length kerma estimator (12). The methodology used to calculate the air-kerma strength has been the same one used in previous studies by our group (7–9). Up to 10^8 photon histories

Fig. 2. Photograph of the vertical (left) and horizontal (right) 3 cm in diameter Leipzig applicators (H3 and V3).

were simulated for each source to obtain air-kerma strength with a standard deviation ($k = 1$) of $\dot{k}_{air}(y)$ of less than 0.5%.

Dose–rate distributions of sources free in water. An MC study for both sources free in water was done to compare the dose–rate distribution with previously published results (13, 14) to validate the user algorithm implemented for this MC application. The sources were located in the center of a spherical water phantom with a 15-cm radius—the same phantom as that used in previous studies (13, 14). A 400 × 800 grid system, composed of 0.05-cm thick and 0.05-cm high cylindrical rings concentric to the longitudinal source axis, was used to score the dose rate in the form of along and away tables. For these cell sizes, the error introduced by averaging dose over the cell is negligible (11). For each source, 2×10^8 histories were simulated obtaining standard deviations ($k = 1$) of the mean dose rate values of less than 0.5%.

Applicator dose–rate distributions in water. The grid system specified in the previous section to score kerma was used to obtain the applicator dose–rate distribution. The three applicators, with the source traveling perpendicular to the contact surface (V1, V2, and V3), present cylindrical symmetry along the axial axis. The applicators with the source traveling parallel to the contact surface (H1, H2, and H3) do not present cylindrical symmetry. However, the dose–rate distributions delivered by these applicators closely approximate to cylindrical symmetry with respect to z axis. Therefore, if we also take into account that controlling source-guide orientation is not possible in clinical routine, cylindrical symmetry has been assumed. The MC dose rate distributions $D(y, z)$ were obtained for the six applicators as follows.

Applicators were placed in contact with a cylindrical liquid water phantom to represent a typical clinical situation. To evaluate the phantom size influence on the dose–rate distribution, two phantom sizes have been considered: a 10-cm high cylinder with a 10-cm diameter and, another, 20-cm high with a 20-cm diameter. For all six applicators, simulations with both sources ("classic" and v2) have been done. For each applicator, 1×10^9 photon histories were simulated obtaining standard deviations ($k = 1$) of the mean dose rate values of less than 0.5%.

Experimental verification of MC application

The MC GEANT4 code (6) is suitable for use in brachytherapy applications (7–9, 15). However, to validate this specific application and to guarantee that realistic source-applicator geometry has been considered, an experimental verification procedure was included in this study, in accordance with the TG43U1 (5) recommendations. Thermoluminiscent dosimeters (TLD) of the type TLD-100 and a parallel-plate ionization chamber were used in a polymethyl methacrylate (PMMA) phantom composed of attached slabs with a total size of 20 × 20 × 6.5 cm^3. Irradiations were performed using an afterloader with a "classic" HDR source. The air-kerma strength S_k was measured using a specific insert inside the well chamber HDR-1000 (Standard Imaging Inc., Middleton, WI) with an electrometer: Max-4000 (Standard Imaging), calibrated at Accredited Dosimetry Calibration Laboratory (ADCL) Wisconsin traceable to National Institute of Standards and Technology (NIST).

To compare experimental results with those obtained by the MC method, a MC study of the "classic" HDR source and applicators in the PMMA phantom was carried out. For this simulation, the same electromagnetic processes and the same cutoff energy and grid system as described previously were considered. Up to 2×10^8 histories were simulated obtaining standard deviations ($k = 1$) of the mean dose–rate values of less than 1%. The MC results were integrated to match the detector volumes.

Thermoluminescent dosimeter measurements. The TLD system used here consists of a Harshaw 6600 TLD reader, together with Harshaw XD-100 extremity (EXT-RAD) dosimeters. The reader employs a hot gas heating technique. Optimum heating cycle parameters were determined as follows: preheat temperature, 160°C; preheat time, 9 s; temperature rate, 12°C/s; maximum temperature, 300°C; acquire time, 30 s; anneal temperature, 300°C; and anneal time, 33 s. After readout, dosimeters were kept at room temperature for 2 h followed by heating at 80°C for 18 h.

The thermoluminescent elements are LiF:Mg,Ti (TLD-100) hot pressed chips, with an area of 3 × 3 mm^2 and a thickness of 100 mg/cm^2 (0.38 mm). The chip is hermetically bonded to a substrate, to which a unique barcode label is attached for identification purposes.

The reader calibration was done using dosimeters chosen at random from the same batch. Those dosimeters were irradiated at ^{60}Co energies and known doses around 500 mGy. Calibration dosimeters were read and annealed together with the rest of the batch. The response of individual dosimeters was corrected for differences in their relative sensitivity, using an element correction factor determined by previous measurements of the whole batch to a common dose.

For each of the six applicators, dosimeters were irradiated at central axis depths of 3.3, 5.85, 8.6, and 11.25 mm with one dosimeter at each depth. This procedure was repeated seven times to evaluate the uncertainties at each measurement point. The doses to the dosimeters range from 10 to 32 cGy for an irradiation time of 17 s. The transit source dose was evaluated measuring the dose at fixed point with the ionization chamber (described in the following section) for various dwell times obtaining that the transit dose is negligible. The length parameter (the distance from the source to the indexer of the microSelectron-HDR) used was 815 mm (16).

To correct the experimental TLD readings for the overresponse of TLD at low energies, the energy spectrum in the PMMA phantom was estimated by means of the MC method. With the energy spectrum obtained at each dosimeter position and the TLD-100 dependence with energy data, provided by Pradhan *et al.* (17), correction factors from energy dependence of the LiF dosimeters were calculated. This reading correction factor is only about

2.5% in relation to the reading given by the dosimeters calibrated in ^{60}Co.

Ionization chamber measurements. In addition to TLD verification, measurements with an ionization chamber were done at a depth of 3 mm in the PMMA phantom. The chamber used was a 0.055 cm^3 Markus parallel-plate ionization chamber (PTW Freiburg), whose active volume is a cylinder 2.7 mm in radius and 2 mm in height. The charge was integrated in an electrometer: Dosimentor DL4/DI4. The effective measurement point of the chamber is at the inner side of the front wall with a thickness of 0.87 mm, equivalent to 1 mm in water (18). To compare this with MC results, a cylindrical cell with the active chamber dimensions was used to score the dose. Cross-calibration of the chamber was done with a cobalt unit. No energy correction was applied (4).

RESULTS AND DISCUSSION

Air-kerma strength for the ^{192}Ir sources

The air-kerma strength found for these sources are (9.86 ± 0.03) × 10^{-8} U/Bq for the "classic" source and (9.81 ± 0.03) × 10^{-8} U/Bq for the v2 source. These values have been compared with those obtained by Borg and Rogers (19) and the differences are 0.7% and 0.8% for the "classic" and v2 sources, respectively.

MC dose–rate distributions in liquid water

The MC calculations for both sources free in a liquid water medium have been compared with well-established published references—MC calculations made by Williamson and Li (13) for the "classic" source and Daskalov *et al.* (14, 20) for the v2 source—showing very good agreement (differences of less than 1% at almost all points). This result ensures that the MC algorithm implemented in the present application is correct.

Monte Carlo simulations in a liquid water medium have been performed for the six applicators with the two different source models available for the microSelectron-HDR, using two representative phantom sizes. Figure 3 shows the phantom size influence (obtained using a 10-cm high cylinder with a 10-cm diameter and, another, 20-cm high with a 20-cm diameter) on dose–rate distributions for H1, H2, and H3 central axis applicators. It can be seen that the differences are only significant beyond a depth of 5 cm, increasing in accordance with the applicator diameter, as was expected. Therefore, a 20-cm high cylinder with a diameter of 20 cm was selected as the typical phantom to calculate dose–rate distributions of the whole set of applicators.

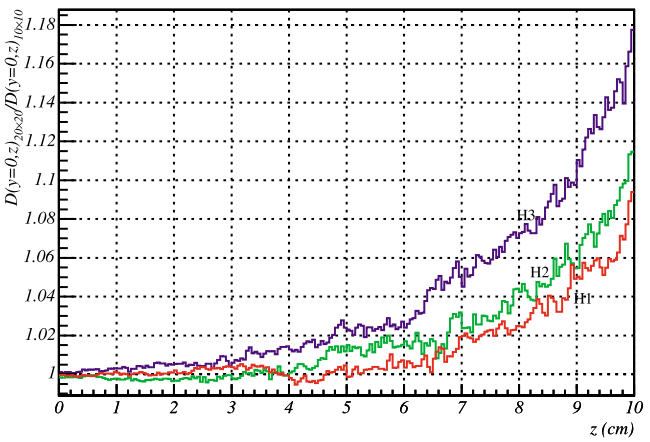

Fig. 3. Ratio between the dose rates along central axis obtained with 20 cm and 10 cm phantom sizes for the H1, H2, and H3 applicators.

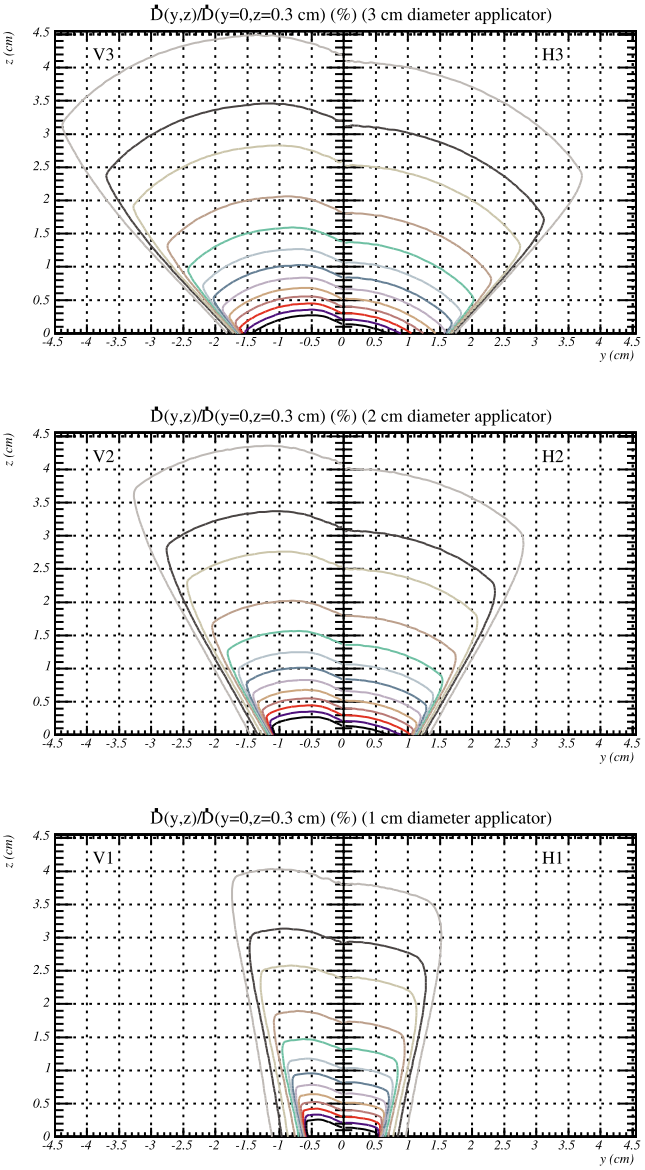

Fig. 4. Relative isodose lines normalized to the dose at a depth of 0.3 cm in the central axis for the horizontal-type (H1, H2, and H3) (right) and vertical-type (V1, V2, and V3) (left) applicators with diameter 1, 2, and 3 cm, respectively, and the v2 source. These are obtained by Monte Carlo calculation for a cylindrical water phantom 20 cm in diameter and 20 cm in height. The isodose curves are 120, 110, 100, 90, 80, 70, 60, 50, 40, 30, 20, 15, and 10%.

In Fig. 4, isodose values normalized to the dose at a depth of 0.3 cm are shown for the six applicators and the v2 source, for which numerical data are included (supplementary material can be found at http://www.uv.es/braphyqs). In Fig. 5, the absolute dose rate per unit kerma strength for

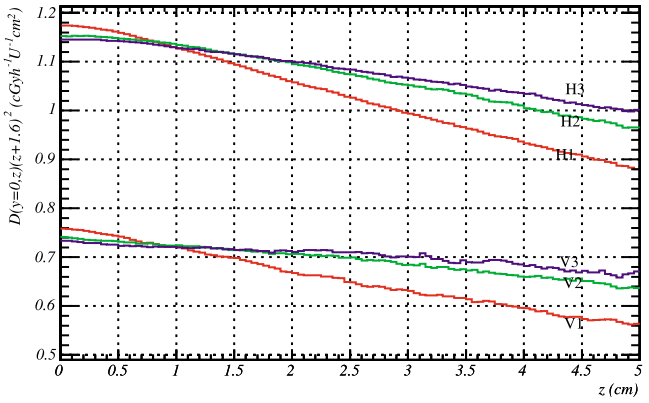

Fig. 5. Dose rate along the applicator central axis for the six applicators with the geometrical dependence (z + 1.6) removed (1.6 cm is the distance from the source center to the skin surface).

the six applicators in the parallel (H1, H2, and H3) and the perpendicular (V1, V2, and V3) configuration, with geometrical dependence removed, are presented for the v2 source. It can be seen that when the applicator diameter decreases, the dose near the applicator surface increases because of wall scatter, whereas at larger depths, it decreases because of the reduction of scatter in water. In Table 1, output factors for the six applicators are presented. These output factors are defined as the dose in $cGyh^{-1}U^{-1}$ in the central axis of the applicator at a depth of 0.3 cm. The comparison of the dose–rate distributions obtained with PMMA and liquid water shows that the output factor changes by about 3%.

The dose–distribution differences between the "classic" and the v2 source are less than 1.5% for the V-type applicators and less than 0.5% for the H-type applicators.

Experimental validation of the GEANT4 code simulation

Figure 6 shows the dose calculated by means of MC and the dose experimentally measured for validation using TLD dosimeters and a parallel plate chamber at different points along the applicator axis. All of them were obtained for a 20 × 20 × 6.5 cm^3 PMMA phantom. The experimentally obtained dose in the PMMA phantom is in good agreement with the dose obtained by means of the MC GEANT4 code calculations. Thus it can be concluded that GEANT4 is validated for this application and that the geometrical design used to describe the Leipzig applicators is suitable.

Table 1. Output factors, per unit kerma strength, for the six applicators and the v2 source at 3-mm depth on the applicator central axis

	Dose at 3-mm depth $cGy/(h^{-1}U^{-1})$
H1	0.325
H2	0.320
H3	0.318
V1	0.208
V2	0.204
V3	0.202

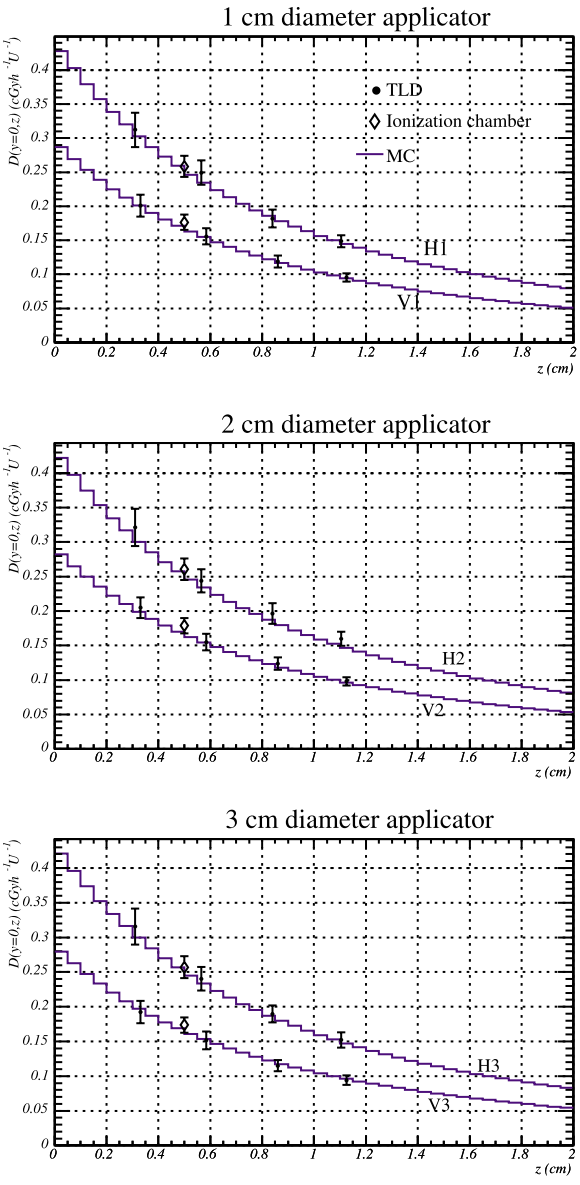

Fig. 6. Comparison of Monte Carlo calculations (full lines), (full circles), thermoluminescent dosimeter and parallel plate ionization chamber (diamond) dose–rate results along the central axis, all of them obtained for a 20 × 20 × 6.5 cm^3 polymethyl methacrylate phantom.

The systematic uncertainties of the TLD measurements were estimated assuming an uncertainty of a 2.3% for the calibration of TLD dosimeters with ^{60}Co and an uncertainty of 3% for the measurement of air-kerma strength with a well chamber. The uncertainties caused by inaccuracy in the positioning of the HDR source in the applicator were estimated at 4–5%. These estimations were made with the aid of MC calculations. The statistical uncertainties from successive measurements with TLD are 3–6%. The quadrature sum of all of these uncertainties gives a global uncertainty of 6–8%.

Comparison of dose–rate distributions with other studies in the literature

It is difficult to compare the results of the present study with those of Evans *et al.* (4) and Huang *et al.* (2), because

they do not present details of uncertainties and agreement between the measurements performed with the different detectors, nor do they gave numerical values of their dose–rate distributions that could be used in clinical practice. Both cited studies conclude that the percentage depth dose along the central axis is nearly the same for all six applicators. However, the results presented in this study indicate greater differences between the percentage depth dose of the six applicators than reported by Evans *et al.* and Huang *et al.*, as can be seen in Fig. 5. These differences reach as high as 5% at $z = 1$ and 20% at $z = 5$.

The comparison of output factors with previous studies has been done in a relative rather than absolute way. This is because the output factors presented by Evans *et al.* are normalized to the H3 applicator and those given by Huang *et al.* are relative to the dose delivered by a ^{192}Ir source at the same distance as a Leipzig applicator in a solid phantom. In the latter case, the setup is not clearly defined. With this restriction in mind, the comparison with the previously published results shows good agreement (1%) for the H-type applicators, but differences of about 25% for the V-type, in which the positioning of the source significantly affects results (about 10% for each mm). As the manufacturer recommends, output dose measurements for the V-type applicator should be performed before use, because the fabrication tolerance when inserting the tube inside the tungsten cap directly affects the source-surface distance, which in turn influences output.

CONCLUSIONS

In this study, tabulated dose rate distributions for Leipzig applicators were obtained using the MC GEANT4 code. The study includes both source types used with the microSelectronHDR: the "classic" source with a 1.1-mm external diameter and the v2 source with a 0.9-mm diameter. These are used in conjunction with the six Leipzig applicators, which have an internal diameter of 1, 2, and 3 cm, with sources parallel or perpendicular to the contact surface.

This application has been validated and realistic geometry guaranteed by means of experimental verification with TLD and a parallel-plate ionization chamber for the six applicators and the "classic" HDR source.

Percentage depth dose and off-axis profiles normalized to a depth of 3 mm on the applicator central axis were obtained. A table of output factors at that depth is presented, normalized to 1 U of the source kerma strength. An air-kerma strength simulation in air has been performed to obtain these data. Correction factors for output measurements when converting from PMMA to liquid water are obtained. The phantom size becomes noticeable at depths greater than 5 cm.

The obtained matrix data, with a grid separation of 0.5 mm, can be used to construct a dataset in a convenient format to allow the modeling of these distributions in a treatment planning system.

These datasets provide the required dosimetry information needed for clinical treatment planning.

REFERENCES

1. Evans MD, Podgorsak EB, Pla M, *et al.* Dosimetric characteristics of surface applicators for high dose-rate brachytherapy [Abstract]. *Med Phys* 1995;22:671.
2. Hwang IM, Leung HWC. Dosimetry characteristics of Leipzig applicators. In: Mould RF, Gurtler MW, editors. Proceedings of the 1st Far East Radiotherapy Treatment Planning Workshop. Veenendaal, The Netherlands: Nucletron-Oldelft; 1996. p. 88–89.
3. Hwang IM, Lin SY, Lin LC, *et al.* Alternative effective modality of Leipzig applicator with an electron beam for the treatment of superficial malignancies. *Nuc Inst Meth A* 2003; 508:460–466.
4. Evans MDC, Yassa M, Podgorsak EB, *et al.* Surface applicators for high dose rate brachytherapy in AIDS-related Kaposi's sarcoma. *Int J Radiat Oncol Biol Phys* 1997;39:769–774.
5. Rivard MJ, Coursey BM, DeWerd LA, *et al.* Update of AAPM Task Group no. 43 report: A revised AAPM protocol for brachytherapy dose calculations. *Med Phys* 2004;31:633–674.
6. Agostinelli S, Allison J, Amako K, *et al.* Geant4—a simulation toolkit. *Nuc Ins Meth A* 2003;506:250–303.
7. Pérez-Calatayud J, Granero D, Ballester F, *et al.* Monte Carlo dosimetric characterization of the Cs-137 selectron/LDR source: Evaluation of applicator attenuation and superposition approximation effects. *Med Phys* 2004;31:493–499.
8. Pérez-Calatayud J, Granero D, Casal E, *et al.* Monte Carlo and experimental derivation of TG43 dosimetric parameters for CSM-type Cs-137 sources. *Med Phys* 2005;32:28–36.
9. Ballester F, Granero D, Perez-Calatayud J, *et al.* Monte Carlo dosimetric study of Best Industries and Alpha Omega Ir-192 brachytherapy seeds. *Med Phys* 2004;31:3298–3305.
10. Wang R, Li XA. A Monte Carlo calculation of dosimetric parameters of ^{90}Sr/^{90}Y and ^{192}Ir SS sources for intravascular brachytherapy. *Med Phys* 2000;27:2528–2535.
11. Ballester F, Hernández C, Pérez-Calatayud J, *et al.* Monte Carlo calculation of dose rate distributions around ^{192}Ir wires. *Med Phys* 1997;24:1221–1228.
12. Williamson JF. Monte Carlo evaluation of kerma at a point for photon transport problems. *Med Phys* 1987;14:567–576.
13. Williamson JF, Li Z. Monte Carlo aided dosimetry of the microselectron pulsed and high dose-rate ^{192}Ir sources. *Med Phys* 1995;22:809–819.
14. Daskalov GM, Löffler E, Williamson JF. Monte Carlo-aided dosimetry of a new high dose-rate brachytherapy source. *Med Phys* 1998;25:2200–2208.
15. Pérez-Calatayud J, Granero D, Ballester F. Phantom size in brachytherapy source dosimetric studies. *Med Phys* 2004;31: 2075–2081.
16. Leipzig Applicators Instruction Manual. Nucletron; 2004.
17. Pradhan AS, Quast U. In-phantom response of LiF TLD-100 for dosimetry of ^{192}Ir HDR source. *Med Phys* 2000;27:1025–1029.
18. Instruction manual for Markus-chamber type 23343. PTW-Freiburg (Physikalisch-Technische Werkstaetten Dr. Pychlau GMBH). Freiburg, Germany; 1987.
19. Borg J, Rogers DWO. Spectra and air-kerma strength for encapsulated ^{192}Ir sources. *Med Phys* 1999;26:2441–2444.
20. Daskalov G. Erratum: Monte Carlo-aided dosimetry of a new high dose-rate brachytherapy source. *Med Phys* 2000;27:1999.